International Journal of Plastics Technology (June 2019) 23(1):77–91
https://doi.org/10.1007/s12588-019-09233-8

RESEARCH ARTICLE

# Modeling of delamination in drilling of glass fiber-reinforced polyester composite by support vector machine tuned by particle swarm optimization

**Ushasta Aich**[1] · **Rasmi Ranjan Behera**[1] · **Simul Banerjee**[1]

Received: 18 August 2018 / Accepted: 23 March 2019 / Published online: 21 May 2019


**Abstract**
Surface damage in machining of fiber-reinforced polymer-based composites is almost unavoidable during manufacturing. Most often, machining operation—drilling causes delamination of composite surface that leads to the loss of quality of product. As a consequence, reasonably accurate prediction of delamination factor (Fd) of drilled hole emerges as a prerequisite during the product development stage and freezing the design before final production. However, stochastic nature of the response and heterogeneous material properties make the modeling difficult. In this article, one of the most advanced generalized learning-based technologies, support vector machine (SVM) which could read the underlying unseen effect of input factors on response, is applied for regression model developing of drilling response—Fd on glass fiber-reinforced polyester composite. Gaussian radial basis function and $\varepsilon$-insensitive loss function are used as kernel functions and loss function, respectively. Particle swarm optimization (PSO) is modified, and modified PSO is employed to search the optimal combination of internal parameters of SVM for modeling of Fd. Model, thus developed, is validated with follow-up testing data sets. Based on estimated model, optimum input parameters for minimum Fd is further investigated using the procedure of modified particle swarm optimization.

**Keywords** Drilling · GFRP composites · Support vector machine (SVM) · Particle swarm optimization (PSO)

**List of symbols**

| | |
|---|---|
| acc | Accuracy level |
| $b$ | Bias |
| $C$ | Regularization parameter |
| $\text{cog}_{\text{initial}}$, $\text{cog}_{\text{final}}$ | Limits of cognitive acceleration coefficient |
| CV | Coefficient of variation |
| dd | Drill diameter (mm) |
| $D_{\max}$ | Maximum diameter of damaged zone |
| $D_{\text{o}}$ | Nominal diameter of hole |
| $f(\boldsymbol{x})$ | Target function |
| Fd | Delamination factor |
| fr | Feed rate (mm/rev) |
| $g_{\text{best}}$ | Global best position of swarm |
| $\text{iter}_{\max}$ | Maximum iteration |
| $K(x_i, \boldsymbol{x})$ | Kernel function |
| MAPE | Mean absolute percentage error |
| mt | Material thickness (mm) |
| $n$ | Number of particles in swarm |
| $N$ | Number of training data |
| $p^i_{\text{best}}$ | Best position of $i^{\text{th}}$ particle |
| rand | Random number within range (0,1) |
| $\text{soc}_{\text{initial}}$, $\text{soc}_{\text{final}}$ | Limits of social acceleration coefficient |
| ss | Spindle speed (rpm) |
| $v^{\text{k}}_{\text{iter}}$ | Velocity of $k$th particle in iter-th iteration |
| $\boldsymbol{w}$ | Weight vector |
| $\boldsymbol{x}$ | Training input vector |
| $x^{\text{k}}_{\text{iter}}$ | Velocity corrected position of $k$th particle in iter-th iteration |
| $\boldsymbol{y}$ | Training output vector |
| $\bar{\text{y}}$ | Mean of training output set |
| $z$ | Number of attributes |
| $\varepsilon$ | Radius of loss insensitive hyper-tube |
| $\eta_{\text{i}}$, $\eta_{\text{i}}^*$, $\alpha_{\text{i}}$, $\alpha_{\text{i}}^*$ | Lagrange multipliers |
| $\xi_{\text{i}}$, $\xi_{\text{i}}^*$ | Slack variables |

✉ Ushasta Aich
ushasta@yahoo.co.in

Simul Banerjee
simul_b@hotmail.com

[1] Mechanical Engineering Department, Jadavpur University, Kolkata 700032, India

| | |
|---|---|
| $\sigma$ | Standard deviation of radial basis function (kernel function) |
| $\sigma_t$ | Standard deviation of training output set |
| $\Phi(x)$ | Feature space |
| $\Psi_{initial}$, $\Psi_{final}$ | Limits of constriction factor |
| $\omega_{initial}$, $\omega_{final}$ | Limits of inertial factor |

## Introduction

In today's competitive market, composites have become one of the mostly used materials in manufacturing industries due to their certain unique advantageous structural and thermal properties. They provide high strength and specific stiffness, high damping, good resistance against corrosion, high fatigue strength, high volume-to-weight ratio, resistance to chemical and microbiological attacks, low thermal conductivity, low thermal expansion, etc. [1]. A wide variety of composites are used for specific purposes in automotive and aviation industries, marine bodies, storage containers, pipes and industrial floorings. In aerospace industries, glass fiber-reinforced plastics are used in fairings, landing gear doors, storage room doors and passenger compartments. Machining processes are used generally to cut, drill and contour composite for building products. Hole making operations are essential for final assembly. It was reported that over 10,000 holes are made in small single engine aircraft while in large transport aircraft, millions of holes are made, most for fasteners—rivets, bolts and nuts which consume almost 50% of total airframe production cost in airframe assembly [2]. Therefore, precise machining needs to be performed to ensure dimensional and functional stability and to obtain a better productivity.

Composites are constituted of matrix and disperse phase. Based on different combination of phase materials, a wide variety of composites with various properties are developed to meet the different needs of customers. To get both elastic behavior and rigid structure of product, fiber-reinforced plastic composites are often preferred. Glass may be used as fiber component due to its high-temperature corrosion resistance, inertness to chemical and environmental attacks. Besides, extremely fine fibers of glass show high strength and stiffness compared to its own normal brittle behavior. Similarly, thermosetting plastics are preferable for matrix phase due to their exclusive thermal properties (permanently hard during their formation and do not soften even at high temperature opposed to thermoplastics) and high volume to weight ratio. Covalent cross-links anchor the network chains of thermosetting polymers together to resist vibrational and rotational chain motion at high temperatures which gives harder, stronger and dimensional stability than thermoplastics [3]. Epoxy and polyester are two commonly used thermosetting plastics. Less expensive polyester is chosen from economic point of view, and glass fiber-reinforced polyester (GFRP) becomes a widely used material in engineering application.

Though GFRP composites have a lot of advantageous material properties, it leads to too much extent of manufacturing difficulties. Chips formed during machining of GFRP causes a severe irritation to human skin. Drilling of GFRP is substantially different from that of metal and results in many undesirable effects such as rapid tool wear, rough surface finish and defective subsurface layers caused by cracks and delaminations. Thus, improper choice of cutting parameter combination may lead to deleterious effect on product performance.

Delamination is an inter-ply phenomenon associated with drilling operation causing reduction in structural integrity and poor assembly tolerance [4]. Induced delamination occurs both at the entrance and exit surface of workpiece rendering it to be less strong. Cutting force acting in the peripheral direction is the main cause of the peeled-up delamination (entrance surface), while the thrust force is the main source of the push out delamination (exit surface) [5]. At the beginning of drilling operation, thickness of the laminated composite material is stable to withstand the thrust force and as the tool approaches the exit plane, stiffness provided by the remaining plies may not be enough to bear the thrust force, causing the lamina to separate resulting in delamination. However, such delamination at exit side may be minimized by using back-up plates.

The delamination that occurs during drilling severely influences the mechanical characteristics of the material around the hole. A common measure of delamination factor (Fd) at the entrance of drilled hole is considered as

$$\mathrm{Fd} = \frac{D_{max}}{D_o} \tag{1}$$

where $D_{max}$ and $D_o$ indicate maximum diameter of damaged zone (Fig. 1) and nominal diameter of the hole, respectively. It is obvious that for better performance of product delamination factor should be minimized.

There have been significant contributions in experimental study on drilling characteristics of composites [6]. Khashaba [7] studied the influence of drilling and material variables on thrust force, torque and delamination of five different types E-glass fiber-reinforced thermosetting composites such as continuous winding with filler/polyester, cross winding/polyester, chopped/polyester, woven/polyester, woven/epoxy. Effect of tool geometry and tool material on thrust force and delamination in drilling of glass fiber-reinforced epoxy composites was investigated by Abrao et al. [8]. Influence of tool point geometry on thrust force and delamination in drilling of glass/phenolic-woven fabric composite using cemented carbide drills was studied by Velayudham

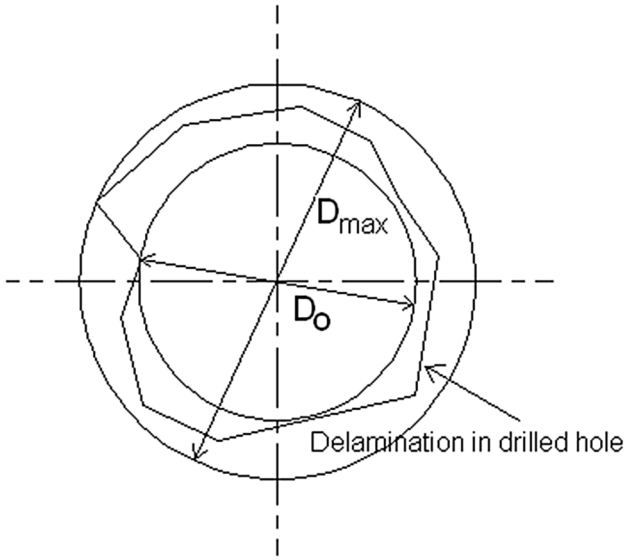


**Fig. 1** Scheme of measuring delamination factor

and Krishnamurthy [9]. EI-Sonbaty et al. [2] suggested that higher cutting speed and fiber volume fraction improve surface roughness of drilled-hole wall of glass fiber-reinforced epoxy composites by conventional high-speed twist drill. Delamination also reduces with increase in cutting speed [10]. Davim et al. [11] used different matrix materials to investigate the cutting characteristics of fiber-reinforced plastic composite materials using cemented carbide drills (K10) with appropriate geometry. Behavior of different drill geometries during machining glass fiber-reinforced plastics was also investigated by Davim et al. [12]. Hocheng and Tsao [13] presented a comprehensive analysis of delamination employing various drill bits such as saw drill, candle stick drill, core drill and step drill.

Various techniques have been applied for modeling and optimization of process parameters to yield lower delamination. Mohan et al. [14] conducted delamination analysis in drilling process of glass fiber-reinforced plastic composite materials using Taguchi's methodology. Palanikumar et al. [15] performed a study on drilling glass fiber-reinforced epoxy composites with two types of cutting tools namely a twist drill and a four flute cutter of high-speed steel using Taguchi's experimental design method as well as response surface methodology. Multivariable linear regression analysis was applied to investigate the effect of the drilling parameters such as speed and feed on cutting forces, thrust and delamination in drilling chopped glass fiber-reinforced epoxy composites with different fiber volume fraction by Khashaba et al. [16]. Multi-layer feed forward ANN architecture trained using error-back propagation training algorithm was used for modeling of delamination in high-speed drilling of carbon fiber-reinforced composite material by Karnik et al. [17]. Stone and Krishnamurty [5] developed a thrust force controller to minimize delamination, and a relationship between feed rate and desired thrust force was modeled by ANN. Multilayered neural network with Levenberg–Marquardt learning algorithm was also employed for the purpose of modeling of drilling responses [18].

Taguchi method and Grey relation analysis were used for optimization of thrust force, surface roughness and delamination factor for GFRP composite by Palanikumar [19] and for carbon fiber-reinforced plastic by Hsu and Tsao [20]. Gaitonde and Karnik [21] developed ANN model for prediction of burr height and burr thickness during drilling of 25-mm-thick AISI 316L stainless steel. They considered multi-response S/N ratio as fitness function for optimization of the two burr size parameters at different drill diameters by PSO. Though their predictive models were tested with small error, the parameters of PSO should be set more accurately to ensure global optimum. Fixed value of cognitive and social acceleration coefficients, termination criteria set by maximum number of iteration value may not guarantee the simulation to reach global optimum. Combining two responses into a single fitness function with equal weight factors may destroy the individual nature of each response. With suitable parameter settings, PSO also requires less time and memory space (small number of function evaluation) to terminate the simulation process. As such, burr formation at the exit side in drilling can be minimized by using back-up materials.

Multivariable regression analysis, response surface methodology and artificial neural network are thus the three main data-based procedures applied for modeling mechanical drilling process of composites. Compared to artificial neural network, support vector machine (a powerful learning system) is devoid of the four problems of efficiency of training, efficiency of testing, over-fitting and algorithm parameter tuning [22]. Besides, the insensitive zone of SVM captures the small-scale random fluctuations appeared in stochastic-type responses which is beneficial for other researchers to apply the models on different products obtained in different batches. An analytic fuzzy logic classification (AFC)-SVM model for tool wear estimation with high accuracy was built by Brezak et al. [23], and Benkedjouh et al. [24] estimated a SVM learned model for remaining useful life (RUL) of cutting tool. Though the models agree with experimental results with less error, no such clear description of the procedure to choose the internal parameters of SVM was reported. Li et al. [25] used WEKA software for prediction of cell vernier through SVM in manufacturing of TFT-LCD. Their developed model gives better prediction than multiple-regression model, but neither the steps of model building nor the simulation procedure for optimal internal parameter settings was

stated. Surface roughness in CNC turning of AISI 304 austenitic stainless steel was modeled with correlation coefficient through three SVM learning systems (LS-SVM, Spider SVM and SVM-KM) and ANN [26]. Parameters of SVM ($C$ and $\sigma$) were set by grid search method. Though it is reported that for model development SVM learning systems consume less time than ANN, no such clear explanation about those specific choices of searching region of SVM parameters was stated. Also, the values of SVM internal parameters obtained through grid search method depend on the choice of jumping interval. However, such predictive model of delamination factor (Fd) in drilling of glass fiber-reinforced polyester composite (GFRP) in particular is not found yet in the literature. Therefore, modeling of response through SVM and optimization of the representative model by PSO are proposed in the present work.

In the present study, experimental results on drilling of glass fiber-reinforced polyester composite with different combinations of input parameters, namely material thickness (workpiece property), drill diameter (cutting tool parameter), spindle speed and feed rate, are taken from thesis work submitted by Behra [27]. Model is developed for delamination factor using structural risk minimization principle-based support vector machine (SVM) learning system. For the purpose of model development, optimum combination of three internal factors in SVM, namely regularization parameter ($C$), radius of loss insensitive hyper-tube ($\varepsilon$) and standard deviation of kernel function ($\sigma$), is searched by modified particle swarm optimization technique. Fitted model is tested through follow-up experiments. The representative model is further used for searching optimal setting of input parameters (material thickness, drill diameter, spindle speed and feed rate) for minimum delamination factor in drilling operation.

## Support vector machine (SVM) [28]

Support vector machine, a supervised batch learning system, is firmly grounded in the framework of statistical learning theory. Vapnik [29] introduced structural risk minimization (SRM) principle instead of empirical risk minimization (ERM), implemented by most of the traditional artificial intelligence-based modeling technologies. Neural network approaches may have suffered with generalization, producing over fitted models but SRM minimizes upper bound on the expected risk, as opposed to ERM, that minimizes error on the training data. This difference equips SVM with a greater ability to generalize [30].

Ultimate goal in modeling of empirical data is to choose a model from hypothesis space, which is closest to the underlying target function. Suppose, a set of training data $\{(x_1, y_1), (x_2, y_2), \ldots. (x_N, y_N)\}$ is used for model developing in d-dimensional input space (i.e., $\mathbf{x} \in R^d$). Key assumption in model developing is that training and testing data set are disjoint, independent and identically distributed according to the unseen but fixed underlying function [22]. The linear target function may be represented in the form [31].

$$f(\boldsymbol{x}) = \langle \boldsymbol{w}, \boldsymbol{x} \rangle + b \tag{2}$$

where $<,>$ indicates dot product in vector space. If the input pattern does not hold any linear relation to output, (nonlinear SVM regression model is shown in Fig. 2), then they are mapped to feature space $\Phi(\mathbf{x})$ from high-dimensional input space via kernel functions. So, optimal choice of weight factor $\mathbf{w}$ and threshold $b$ (bias term) is prerequisite of accurate modeling. Flatness of the model is controlled by minimizing Euclidean norm $\|\mathbf{w}\|$. Besides, empirical risk of training error should also be minimized [32]. So, regularized risk minimization problem for model developing can be written as follows

$$R_{\text{reg}}(f) = \frac{\|\boldsymbol{w}^2\|}{2} + C\sum_{i=1}^{N} L\left(y_i, f\left(\mathrm{x}_i\right)\right) \tag{3}$$

Weight vector $\mathbf{w}$ and the bias term b can be estimated by optimizing this function (Eq. (3)), which minimizes not only empirical risks but also reduces generalization error, i.e., over-fitting of model simultaneously. Here, $L(\mathbf{y})$, a loss function is introduced to penalize over-fitting of model with training points. A number of loss functions are already developed for handling different types of problems [30]. $\varepsilon$-insensitive loss function (Fig. 3) is mostly used for process modeling problems. This function may be defined as

$$\begin{aligned} L(y_i, f(x_i)) &= \left|y_{i,\text{experimental}} - f(x_i)\right| - \varepsilon, \text{ if } \left|y_{i,\text{experimental}} - f(x_i)\right| \geq \varepsilon \\ &= 0, \qquad\qquad \text{if } \left|y_{i,\text{experimental}} - f(x_i)\right| < \varepsilon \end{aligned} \tag{4}$$

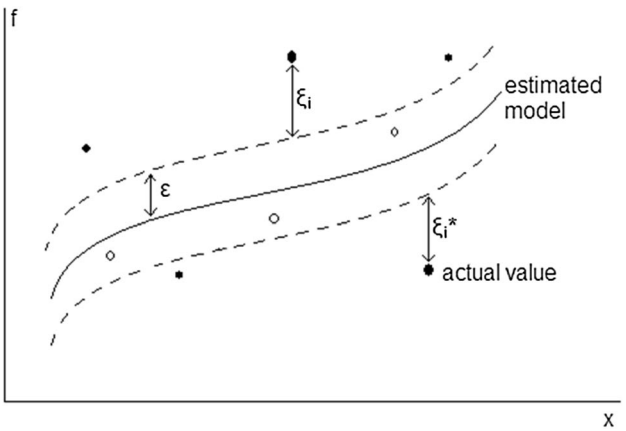


**Fig. 2** Nonlinear SVM regression model

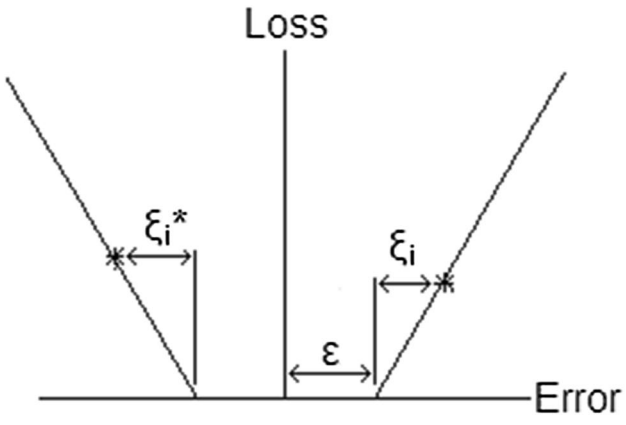


**Fig. 3** $\varepsilon$-Insensitive loss function

Here, points inside the $\varepsilon$-tube are considered as zero loss; otherwise, a penalization is calculated by introducing $C$, which is a trade-off between flatness and complexity of the model. Practical significance of this insensitive zone is that the points inside the hyper-tube, i.e., close enough to estimated model are deemed to be well estimated and those outside the tube contribute training error loss. The outsiders of the insensitive zone belong to support vector group. So, size of $\varepsilon$-insensitive zone controls number of support vectors. As radius of insensitive hyper-tube increases, number of support vector reduces and flexibility of the model diminishes. This behavior may be advantageous for eliminating the effect of small random noise in output, but larger value of $\varepsilon$ will not completely extract the unseen target function. Besides, higher value of $C$ makes the model more complex with the chance of over-fitting, but too small value may increase training errors. So, optimum choice of this regularization parameter is necessary for better modeling. Two positive slack variables $\xi_i$ and $\xi_i^*$ are introduced [29, 31] to cope with infeasible constraints of the optimization problem. Hence, the constrained problem can be reformulated as

$$\begin{aligned} \text{minimize:}\quad & \frac{\|\boldsymbol{w}\|^2}{2} + C\sum_{i=1}^{N}\left(\xi_i + \xi_i^*\right) \\ \text{subject to:}\quad & y_{i,\exp} - \langle \boldsymbol{w}, \boldsymbol{x}\rangle_i - b \le \varepsilon + \xi_i \\ & \langle \boldsymbol{w}, \boldsymbol{x}\rangle_i + b - y_{i,\exp} \le \varepsilon + \xi_i^* \\ & \xi_i,\ \xi_i^* \ge 0, \quad \boldsymbol{i} = 1(1)N \end{aligned} \tag{5}$$

This problem can be efficiently solved by standard dualization principle utilizing Lagrange multiplier. A dual set of variables are introduced for developing Lagrange function. It is found that this function has a saddle point with respect to both primal and dual variables at the solution. Lagrange function can be stated as

$$\begin{aligned} L = {} & \frac{\|\boldsymbol{w}\|^2}{2} + C\sum_{i=1}^{N}\left(\xi_i + \xi_i^*\right) - \sum_{i=1}^{N}\left(\eta_i\xi_i + \eta_i^*\xi_i^*\right) \\ & - \sum_{i=1}^{N}\alpha_i\left(\varepsilon + \xi_i - y_i + \langle \boldsymbol{w}, \boldsymbol{x}\rangle_i + b\xi_i^*\right) \\ & - \sum_{i=1}^{N}\alpha_i^*\left(\varepsilon + \xi_i^* + y_i - \langle \boldsymbol{w}, \boldsymbol{x}\rangle_i - b\right) \end{aligned} \tag{6}$$

where $L$ is the Lagrangian and $\eta_i$, $\eta_i^*$, $\alpha_i$, $\alpha_i^*$ are Lagrange multipliers satisfying $\eta_i$, $\eta_i^*$, $\alpha_i$, $\alpha_i^* \ge 0$. So, partial derivatives of $L$ with respect to $w$, $b$, $\xi_i$, $\xi_i^*$ will give the estimates of $\mathbf{w}$ and $b$. The present problem is solved by using LibSVM MATLAB Toolbox.

Support vectors can be easily identified from the value of difference between Lagrange multipliers ($\alpha_i$, $\alpha_i^*$). Very small values (close to zero) indicate the points inside the insensitive hyper-tube, but nonzero values belong to support vector group [33]. The $\mathbf{w}$ can be calculated by [31]

$$\boldsymbol{w} = \sum_{i=1}^{N}\left(\alpha_i - \alpha_i^*\right)\boldsymbol{\Phi}\left(x_i\right) \tag{7}$$

The idea of kernel function $K(x_i, \mathbf{x})$ gives a way of addressing the curse of dimensionality [30]. It helps to enable the operations to be performed in the feature space rather than potentially high-dimensional input space. A number of kernel functions satisfying Mercer's condition were suggested by researchers [33, 34]. Each of the functions has its own specialized applicability. Gaussian radial basis function with $\sigma$ standard deviation [given in Eq. (8)] is commonly used for its better potentiality to handle higher-dimensional input space.

$$K\left(x_i, \boldsymbol{x}\right) = e^{-\frac{\|x_i - x^2\|}{2\sigma^2}}\Big|_{\sigma_{\text{optimum}}} \tag{8}$$

Thus, the final model with optimum choice of $C$, $\varepsilon$ and $\sigma$ may be presented as [31]

$$f(x) = \sum_{i=1}^{N}\left(\alpha_i - \alpha_i^*\right)K\left(x_i, x\right) + b\Big|_{\substack{C_{\text{optimum}} \\ \varepsilon_{\text{optimum}} \\ \sigma_{\text{optimum}}}} \tag{9}$$

## Particle swarm optimization (PSO) [28]

Particle swarm optimization (PSO) technique is one of the most advanced evolutionary computational intelligence-based optimization methodologies for optimizing real-world multimodal problems. PSO mimics natural behavior

found in flock of birds or school of fish seeking their best food sources [35]. In this population based swarm intelligence technique, a set of randomly initialized particles (swarm) are always updated in position and velocity by gathering information from themselves. Effect of each particle as well as the whole swarm's experience modifies position of the population forwarding to optimum zone. Rate of convergence is purposefully controlled by different factors. Position of global optimum is not affected by the choice of the factors, but convergence is delayed due to improper choice or may lead to entrapping in local optima. For multivariable problem in high-dimensional space, time and memory space needed for reaching optimum solution by PSO are very important.

Number of particles ($n$) in swarm should be within the range (10, 40) [36]. Lower choice may not gather information from whole space, but higher value of n will take longer time to converge in optimum zone.

Inertia factor ($\omega$) controls the effect of previous velocity of individual particle on current velocity. To modify the rate of convergence another control on simulation was done by introducing constriction factor ($\Psi$) [37]. This term bounds the velocity effect of particles on their position avoiding clamping of particles to one end of search space [38]. So, higher values of inertia and constriction factor ensure wide searching which is necessary at initial stage but gradual convergence is enhanced at moderately lower value.

Another two important factors are cognitive acceleration coefficient (cog) and social acceleration coefficient (soc) which greatly control the influence of individual's and whole swarm's experience, respectively, on particle's new velocity. Individual best ($p^i_{\text{best}}$) experience of each particle favors good exploration in the search space but the best position ($g_{\text{best}}$) of swarm always guides to converge near optimum zone. So, choice of the factors becomes important for converging to global optimum zone quickly avoiding premature entrapping in local optima.

Several researchers use different values of the control factors for their different type of problem definitions. However, in general, for most of the cases, nearly a same range is suggested irrespective of the nature of problem [39]. Shi and Eberhart [40] suggested linearly decreasing inertia factor from 0.9 to 0.4. Cognitive acceleration coefficient should vary linearly with iterations from 2.5 to 0.5 while the variation of social acceleration coefficient would occur just in reverse order [41]. Since constriction factor directly controls the optimization time, it may be considered as linearly time varying from 0.9 to 0.4.

Further, maximum number of iterations is to be set properly. A large value is necessary for adequate convergence. In other words, simulation will be terminated before reaching this limiting value.

**Table 1** Parameters and their levels

| | Level 1 | Level 2 | Level 3 |
|---|---|---|---|
| Material thickness (mm) | 8 | 12 | 16 |
| Drill diameter (mm) | 10 | 12 | 14 |
| Spindle speed (rpm) | 400 | 800 | 1100 |
| Feed rate (mm/rev) | 0.100 | 0.175 | 0.275 |

## Experiment [27]

Experiment was conducted on a radial drilling machine (Make: The American Tool Works Co., USA) [27]. The machine is equipped with a maximum spindle speed of 1500 rpm and variable feed from 0.1 to 0.625 mm/rev with a 5.5 kW drive motor. Maximum radial dimension of workpiece is 1475 mm.

In the present study, material thickness (mt), drill diameter (dd), spindle speed (ss) and feed rate (fr) are considered as input parameters and delamination factor (Fd) measured on entrance surface as response parameter for drilling process. Based on the availability of the machine setting, levels of the input parameters are selected and presented in Table 1.

GFRP composite used in the experiment was supplied by VMT Glass Fiber Roofing Industries. Hand lay-up technique is used for producing the composite. Chopped strand mat E-glass fiber is used as reinforcement in polyester resin to prepare the laminate. Mechanical and physical properties of this composite are shown in Table 2. Experiments are carried out on GFRP samples of size 150 mm × 150 mm using wood as backing material.

HSS taper shank twist drills (Make: Addison & Co. Ltd., India) confirming to IS: 5103-1969/ISO: 235-1980/DIN: 345-1978/BS: 328: Part: 1-1986 specifications were utilized for the drilling experiments. Chemical composition of HSS tool material is listed in Table 3. Three different diameter twist drills (shown in Table 4) of grade M2 were employed.

**Table 2** Properties of GFRP composite

| Tensile strength | 700 kg/cm$^2$ |
|---|---|
| Hardness | Barcol 40.5 |
| Matrix | Polyester |
| Reinforcing | E-glass, chopped strand mat (450 g/m$^2$) |
| Volume fraction of glass fiber | 0.33 |
| Hardener | Methyl ethyl ketone peroxide |

**Table 3** Chemical composition of HSS tool material (wt%)

| *C* | Cr | Mo | *W* | *V* |
|---|---|---|---|---|
| 0.9 | 4.2 | 5.0 | 6.4 | 1.8 |

**Table 4** Specifications of twist drills

| Drill diameter (mm) | Flute length (mm) | Overall length (mm) |
|---|---|---|
| 10 | 87 | 168 |
| 12 | 101 | 182 |
| 14 | 108 | 189 |

Damage around the holes at the entrance was measured with a toolmakers' microscope with 30× magnification (Make: Carl Zeiss Ltd.). Delamination factor (Fd) is calculated using Eq. (1).

Among 81 unique combinations of the levels of different input parameters, randomly 11 sets are kept aside for testing purposes and rest 70 data sets are used for training the learning process.

## Analysis and discussion

Model for delamination factor (Fd) is fitted through learning process of SVM based on training data sets. Fitted model is tested through another 11 sets of data. Then the representative model is used for searching optimal combination of input parameters (material thickness, drill diameter, spindle speed and feed rate) for minimum delamination factor (Fd).

### Model development

Significance of parameter selection in SVM for model development and thereby for good prediction is evident. Particle swarm optimization (PSO) could be used effectively for this purpose. The most influencing parameters in SVM learning process are $C$, $\varepsilon$ and $\sigma$. With optimum choice of $C$, $\varepsilon$ and $\sigma$, a set of Lagrange multipliers ($\alpha_i$, $\alpha_i$*) could be found and the model can be estimated using Eq. (9).

At first, search spaces for each of the parameters (C, $\varepsilon$ and σ) are to be determined. A wide range of each parameter may be a good search space, but this will take large computation time. Estimation of C based on experimental outputs (target values) was suggested by Levis and Papageorgiou [34], Cherkassky and Ma [42].

$$C = max\left(\left|\bar{y} + 3\sigma_t\right|, \left|\bar{y} - 3\sigma_t\right|\right) \tag{10}$$

where $\bar{y}$ and $\sigma_t$ represent mean and standard deviation of target values. However, this exact value may lead to erroneous modeling due to the presence of random noises. So, it is better to choose a range for $C$ and searching operation is to be performed within the limits. At first, using Eq. (10) $C$ value is calculated for Fd as $C_{Fd} = 1.4160$. Then, considering normal distribution with mean at this calculated $C$ value and 50% of mean value as standard deviation, two points are chosen at both sides of estimated $C$ value. Thus, range of $C$ for Fd is determined (Table 5).

**Table 5** Searching range of SVM parameters

| SVM parameter | C | $\varepsilon$ | σ |
|---|---|---|---|
| Searching range | [0.2043, 2.7143] | [0.0409, 0.1226] | [0.5623, 0.8409] |

Based on experiments, suitable range of $\varepsilon$ and that of σ are also suggested in [34, 42]. Inside the bounds of σ, generalization performance is found as stable. Those limits can be calculated from

$$\varepsilon = \left[\frac{\bar{y}}{30}, \frac{\bar{y}}{10}\right], \ \sigma = \left[0.1^{\left(\frac{1}{z}\right)}, \ 0.5^{\left(\frac{1}{z}\right)}\right], \tag{11}$$

Here, $z$ indicates number of most influencing attributes in the process. In this study of drilling process, it is four namely material thickness, drill diameter, spindle speed and feed rate. Using Eq. (11), $\varepsilon$ and $\sigma$ values for Fd are calculated (Table 5).

For better implementation of this estimated search range, it was suggested [34, 42] to normalize the training inputs within the range (0, 1). So, the input parameters of drilling process, i.e., material thickness (mt), drill diameter (dd), spindle speed (ss) and feed rate (fr) are normalized using the following formulae.

$$x_{1,\text{norm}} = \frac{\text{mt} - 8}{16 - 8}, \quad x_{2,\text{norm}} = \frac{\text{dd} - 10}{14 - 10},$$
$$x_{3,\text{norm}} = \frac{\text{ss} - 400}{1100 - 400}, \quad x_{4,\text{norm}} = \frac{\text{fr} - 0.100}{0.275 - 0.100} \tag{12}$$

As SVM reduces the chance of generalization error; in the present study, parameters of SVM are selected through minimization of mean absolute percentage error (MAPE) in estimation of training outputs. For the purpose of optimization, MAPE being a function of C, $\varepsilon$ and σ, is considered as the objective function. At every step during marching procedure, different combinations of C, $\varepsilon$ and σ will develop different regression models. For each of the models developed through the change of C, $\varepsilon$ and σ values, MAPE [Eq. (13)] is calculated and searching of minimum MAPE is done among the models using the procedure of particle swarm optimization.

$$\text{MAPE}(\%) = \frac{100}{\text{N}} \sum_{\text{i}=1}^{\text{N}} \left| \frac{\text{y}_{\text{i,experimental}} - \text{y}_{\text{i,estimated}}}{\text{y}_{\text{i,experimental}}} \right| \tag{13}$$

In most of the papers, termination criterion is set by a predefined maximum number of iterations. This may not

ensure global optima. Rather, a statistical measure of relative dispersion, coefficient of variation (CV) of the position of particles in search space, is expected to help avoiding the premature stopping of simulation procedure. Coefficient of variation is calculated as a ratio of standard deviation to mean and expressed in percentage.

$$\text{Coefficient of variation(CV)}(\%) = 100 \times \frac{\text{standard deviation of current position vector}}{\text{mean of current position vector}} \tag{14}$$

A very small value of this criterion indicates a set of densely compact particles in the swarm, irrespective of their search range in different dimensions. Small coefficient of variation in conjunction with negligible change in the values of MAPE will ensure global optimum. Besides, nature of change of different components of CV values in different dimensions may give a preliminary idea about the underlying relationship among output and inputs. Therefore, above proposed modification is introduced and modified PSO algorithm for searching optimum combination of $C$, $\varepsilon$ and $\sigma$ for minimum MAPE is described as follows.

*Step 1* Choose number of particles in swarm (n), maximum number of iterations iter $_{max}$, accuracy level (acc). Set, inertia factor range ($\omega_{initial}$, $\omega_{final}$), cognitive acceleration coefficient range ($cog_{initial}$, $cog_{final}$), social acceleration coefficient range ($soc_{initial}$, $soc_{final}$) and constriction factor range ($\Psi_{initial}$, $\Psi_{final}$).
*Step 2* Set iter = 1. Randomly initialize the position of n particles in swarm that is n set of initial combination of C, $\varepsilon$ and σ. Also randomly set initial velocity of each particle using following relation.

$$v_{iter}^{(i)} = \text{range}^{(i)} \times \text{rand}, \quad i = 1(1)3 \tag{15}$$

where "range$^{(i)}$" and "rand" indicate range of $C$, $\varepsilon$ and $\sigma$ (shown in Table 5) and a random number within the range (0,1), respectively. So, $n$ set of velocity vectors with components along $C$, $\varepsilon$ and $\sigma$ coordinates are initialized.
*Step 3* Set t = 1 and $p_{best}^{t}$ and $g_{best}$ as current position vector.
*Step 4* Check whether $t = n$ or not. If yes go to step 8, otherwise set $t = t + 1$ and go to step 5.
*Step 5* Calculate MAPE (objective function value) at $t$th particle position in swarm using Eq. (13). If iter = 1, then set $p_{best}^{t}$ as current position vector and go to step 7. Otherwise, go to step 6.
*Step 6* If this MAPE value is smaller (better) than MAPE at already set $p_{best}^{t}$, then update $p_{best}^{t}$ vector. Otherwise, $p_{best}^{t}$ is kept unaltered.
*Step 7* Check whether this current MAPE value is lesser (better) than MAPE at already set $g_{best}$. If yes, update $g_{best}$ vector to current position vector and go to step 4. Otherwise, $g_{best}$ vector is kept unaltered and go to step 4.
*Step 8* Calculate coefficient of variation of particles' position in current swarm using Eq. (14). Each position vector has three components along $C$, $\varepsilon$ and $\sigma$. So, three values of coefficient of variation will be found.
*Step 9* If all the three coefficient of variation values simultaneously become less than accuracy level, then terminate the simulation process and go to step 14, otherwise set $k = 1$ and go to step 10.
*Step 10* Considering linear gradient of $\omega$, $cog$, soc and $\Psi$, set the value of the control factors for this iteration (iter) using the following relations.

$$\begin{aligned}
\omega_{iter} &= \omega_{initial} + \frac{(\omega_{final} - \omega_{initial})}{(\text{iter}_{max} - 1)}(\text{iter} - 1)\\
\text{cog}_{iter} &= \text{cog}_{initial} + \frac{(\text{cog}_{final} - \text{cog}_{initial})}{(\text{iter}_{max} - 1)}(\text{iter} - 1)\\
\text{soc}_{iter} &= \text{soc}_{initial} + \frac{(\text{soc}_{final} - \text{soc}_{initial})}{(\text{iter}_{max} - 1)}(\text{iter} - 1)\\
\psi_{iter} &= \psi_{initial} + \frac{(\psi_{final} - \psi_{initial})}{(\text{iter}_{max} - 1)}(\text{iter} - 1)
\end{aligned} \tag{16}$$

*Step 11* Update $k$th particle's velocity vector and its velocity corrected position vector using the following formulae.

$$\begin{aligned}
v_{(m)iter+1}^{k} &= \omega_{iter}\left(v_{(m)iter}^{k}\right) + c_{1,iter}(\text{rand})\left(p_{(m)best}^{k} - x_{(m)iter}^{k}\right)\\
&\quad + c_{2,iter}(\text{rand})\left(g_{(m)best} - x_{(m)iter}^{k}\right)\\
x_{(m)iter+1}^{k} &= x_{(m)iter}^{k} + \Psi\left(v_{(m)iter+1}^{k}\right),\ m = 1(1)3
\end{aligned} \tag{17}$$

*Step 12* If new positions of particles ($C$, $\varepsilon$ and $\sigma$) go outside the specified search range (shown in Table 2), then reset its current position to the violating limit. If $k = n$, then go to step 13. Otherwise set $k = k + 1$ and go to step 11.
*Step 13* If iter = iter$_{max}$, then go to step 1 and restart the simulation with larger iter$_{max}$, such that termination criterion will be satisfied before reaching that new limit. Otherwise set iter = iter + 1 and $t = 1$, go to step 5.
*Step 14* Set current $g_{best}$ of the swarm as optimum point, i.e., components of latest $g_{best}$ vector become the optimum combination of $C$, $\varepsilon$ and $\sigma$ for minimum MAPE in fitting the regression model on training data.

Therefore, final $g_{best}$ vector satisfying the termination criterion becomes global optimum in that specified search space. The flow chart for searching optimum parameter

combination ($C$, $\varepsilon$ and $\sigma$) of SVM through modified PSO by minimizing MAPE of training data is also shown in Fig. 4.

In the present work, different control factors of modified PSO are set as, number of particles in swarm ($n$) = 20, $\omega_{initial} = 0.9$, $\omega_{final} = 0.4$, $cog_{initial} = 2.5$, $cog_{final} = 0.5$, $soc_{initial} = 0.5$, $soc_{final} = 2.5$, $\Psi_{initial} = 0.9$, $\Psi_{final} = 0.4$, $iter_{max} = 250$, accuracy level (acc) = 1.0 (i.e., simulation will stop when each component of coefficient of variance of particles' position goes down below 1%).

As PSO is a population-based searching technique; a proper choice of initial positions vectors of the particles within specified search space and their corresponding velocities are to be set randomly. But wide spreading of initial position vectors must be assured by the operator for better searching. The set

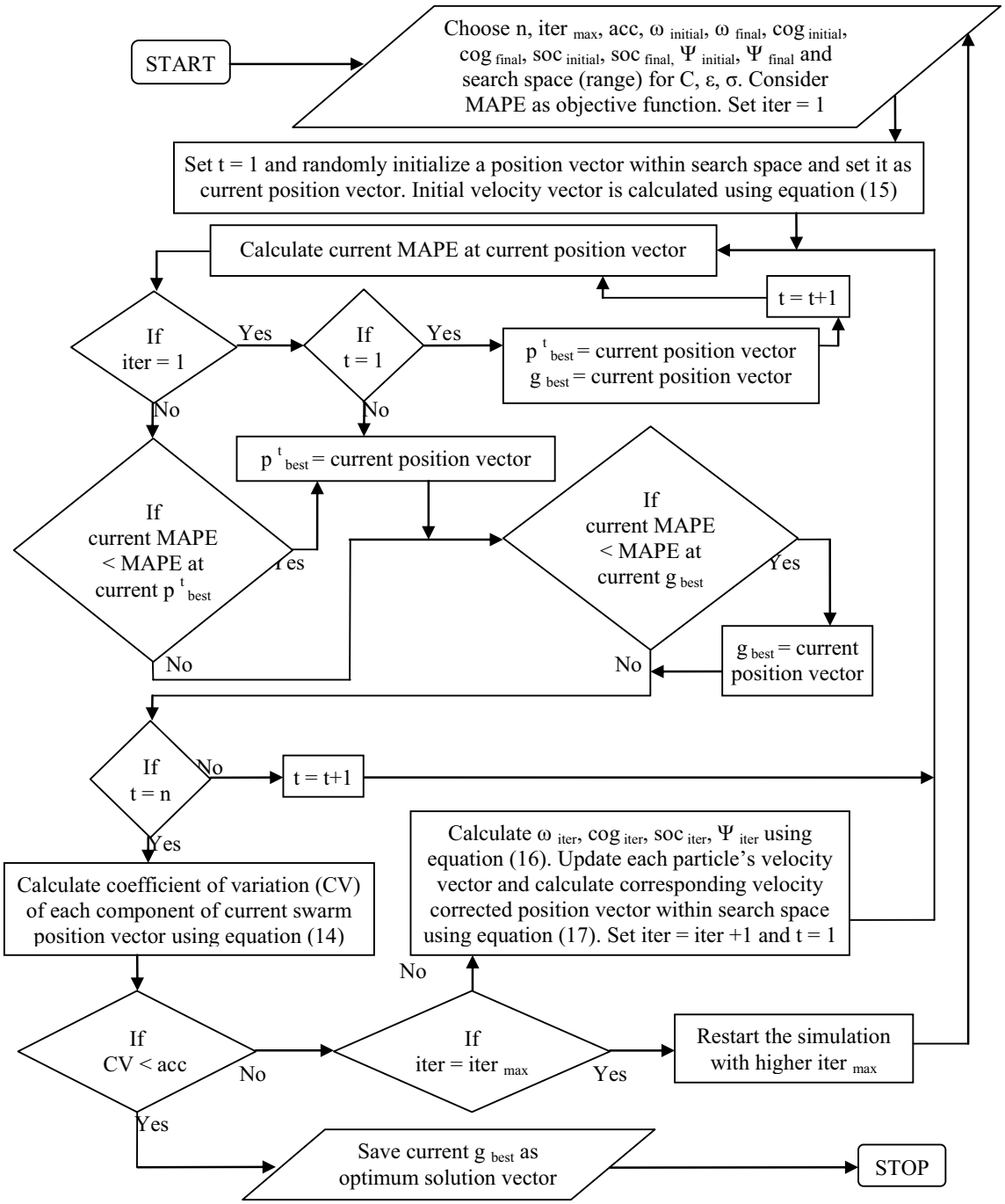


**Fig. 4** Flow chart for searching optimum combination of C, $\varepsilon$ and σ through modified PSO by minimizing MAPE of training data

of values should be memorized by the computing machine for exact repetitiveness of the simulation process.

Different combinations of $C$, $\varepsilon$ and $\sigma$ change the shape of model, and best fitted model will have minimum fitting error that is minimum MAPE. As such the MAPE of the fitted model should be minimized. In this study, best fitted model with minimum MAPE is constructed on optimum combination of $C$, $\varepsilon$ and $\sigma$ that is the best position of the particles in swarm.

Thus optimizing MAPE by modified PSO with the initial position and velocity vectors, a set of $C$, $\varepsilon$ and $\sigma$ for Fd is found (shown in Table 6). Marching steps of the simulation process for minimizing MAPE are shown in Fig. 5. Though MAPE values remain unchanged after some iteration, yet the simulation is continued further. In this work, termination criterion is set by CV of position vectors' components along each dimension ($C$, $\varepsilon$ and $\sigma$), as this will ensure proper convergence of the searching operation to optimum zone. So, iteration process is continued until coefficient of variation of position vector components in each dimension ($C$, $\varepsilon$ and $\sigma$) goes down below 1% (refer Fig. 6) although MAPE remains unchanged. Coefficient of variation (expressed in %) of position vectors in different dimensions is calculated by taking the ratio of standard deviation to mean of position vector component along respective dimensions.

Figure 6 indicates that effect of $C$ is lower than $\varepsilon$ and $\sigma$ as CV for $C$ dies out at a slower rate. This may conclude that model of Fd is not too much sensitive to the value of $C$. But rapid die down nature of $\varepsilon$ and $\sigma$ gives a strong evidence in favor of the presence of random noises in the responses.

**Table 6** Optimum SVM parameters and training error measurement

| C | $\varepsilon$ | σ | MAPE |
|---|---|---|---|
| 2.1569 | 0.0409 | 0.8409 | 2.1405 |

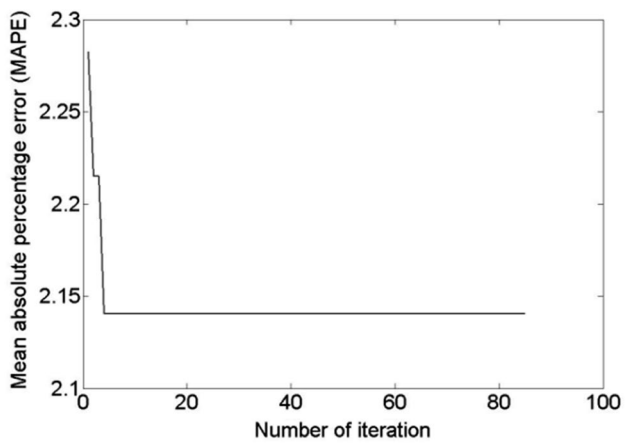


**Fig. 5** Marching steps for optimization of MAPE for modeling of Fd

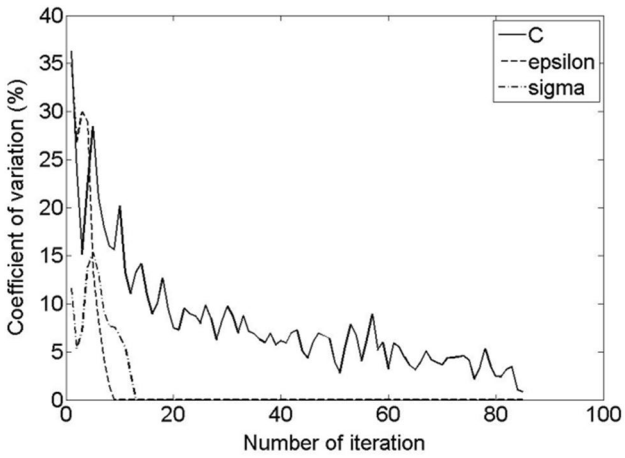


**Fig. 6** Change of CV with iterations for optimization of MAPE for modeling of Fd

Optimum $C$ and $\varepsilon$ values are found near the upper and lower bound of search space, respectively. Higher value of $C$ (with respect to specified search space) signifies that the model of Fd is highly complex in nature with large random noises. This gives a good indication in favor of the stochastic nature of drilling composite material. The random noises in the output of this stochastic process are fairly controlled in developing a model by SVM with proper choice of $\varepsilon$. Process outputs within $\varepsilon$-tube do not greatly affect the complexity of model. Here lower value of $\varepsilon$ for indicates that the estimated model capture small-scale randomness adequately. Besides, higher value of $\sigma$ captures the oscillatory nature of training data which are not penalized by $\varepsilon$-insensitive zone. In the present study, optimum $\sigma$ shifts toward upper end that is there is an oscillatory pattern outside the insensitive tube.

With the estimated optimum combination of $C$, $\varepsilon$ and $\sigma$, Lagrange multipliers ($\alpha_i$, $\alpha_i^*$) are calculated (shown in Table 9) and the developed model for Fd can be represented as

$$\text{Fd:}\quad f(x) = \sum_{i=1}^{N} \left(\alpha_i - \alpha_i^*\right) K\left(x_i, x\right) + b \Big|_{\substack{C = 2.1569 \\ \varepsilon = 0.0409 \\ \sigma = 0.8409}}$$

$$\text{with } K\left(x_i, x\right) = e^{-\frac{x_i - x^2}{2\sigma^2}} \Big|_{\sigma = 0.8409}$$

To depict the effect of different input parameters (material thickness, drill diameter, spindle speed and feed rate) on delamination factor, surface plots are generated using the above estimated model. The representative surface plots are shown in Figs. 7, 8, 9, 10, 11 and 12. Feed rate is observed a significant factor.

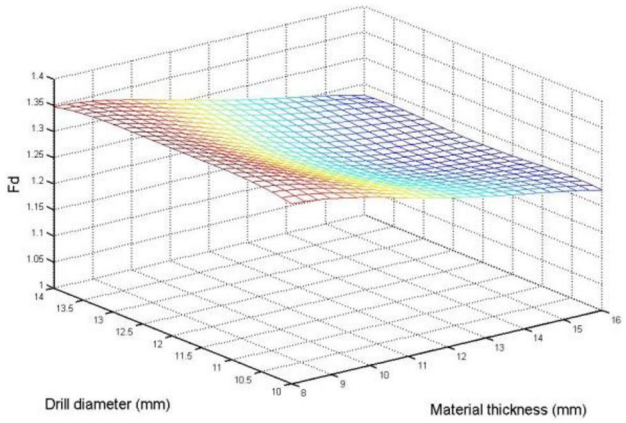


**Fig. 7** Effect of material thickness & drill diameter on Fd at ss = 750 rpm & fr = 0.1875 mm/rev

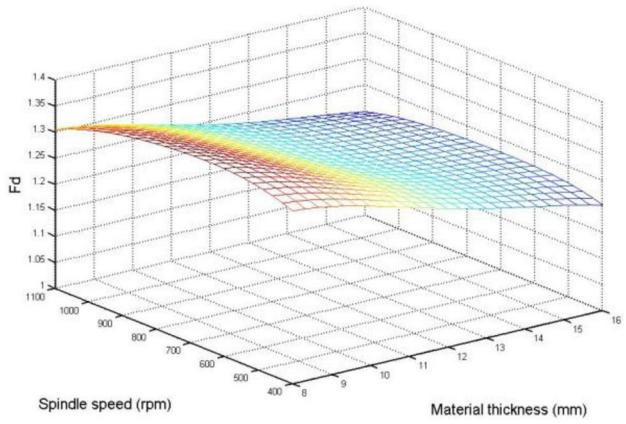


**Fig. 8** Effect of material thickness & spindle speed on Fd at dd = 12 mm and fr = 0.1875 mm/rev

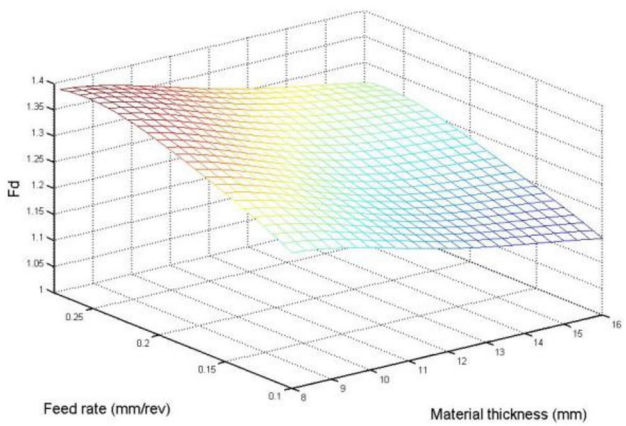


**Fig. 9** Effect of material thickness & feed rate on Fd at dd = 12 mm and ss = 750 rpm

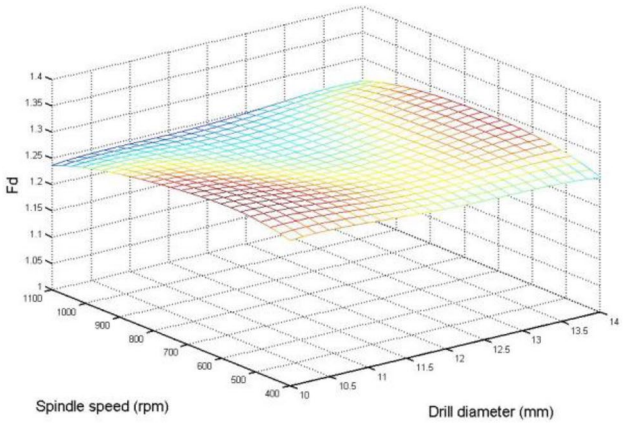


**Fig. 10** Effect of drill diameter & spindle speed on Fd at mt = 12 mm and fr = 0.1875 mm/rev

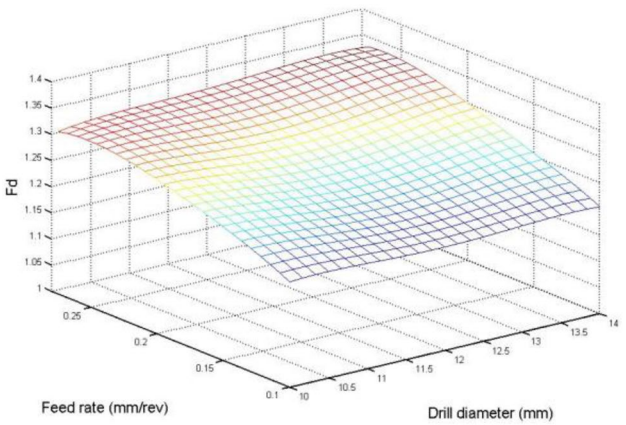


**Fig. 11** Effect of drill diameter & feed rate on Fd at mt = 12 mm and ss = 750 rpm

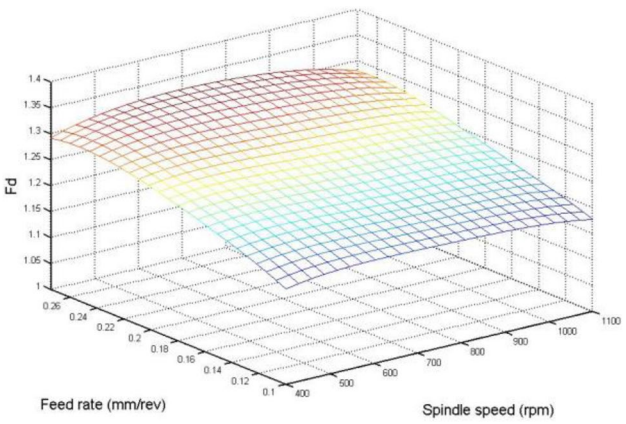


**Fig. 12** Effect of spindle speed & feed rate on Fd at mt = 12 mm & dd = 12 mm

**Table 7** Testing for Fd

| Sl. No. | Material thickness (mm) | Drill diameter (mm) | Spindle speed (rpm) | Feed rate (mm/rev) | Fd (experimental) | Fd (estimated) | Absolute % error |
|---|---|---|---|---|---|---|---|
| 1 | 8 | 10 | 800 | 0.175 | 1.2622 | 1.3294 | 5.3230 |
| 2 | 8 | 12 | 800 | 0.175 | 1.2844 | 1.3438 | 4.6225 |
| 3 | 8 | 14 | 400 | 0.175 | 1.2692 | 1.2867 | 1.3802 |
| 4 | 8 | 14 | 800 | 0.175 | 1.2762 | 1.3335 | 4.4921 |
| 5 | 12 | 10 | 800 | 0.175 | 1.2058 | 1.2724 | 5.5204 |
| 6 | 12 | 12 | 400 | 0.175 | 1.1945 | 1.2566 | 5.1951 |
| 7 | 12 | 12 | 1100 | 0.175 | 1.2197 | 1.2346 | 1.2199 |
| 8 | 16 | 10 | 400 | 0.175 | 1.1893 | 1.1993 | 0.8448 |
| 9 | 16 | 10 | 1100 | 0.175 | 1.1743 | 1.1655 | 0.7480 |
| 10 | 16 | 12 | 800 | 0.175 | 1.1841 | 1.2136 | 2.4929 |
| 11 | 16 | 14 | 800 | 0.175 | 1.1867 | 1.2182 | 2.6532 |
| Mean absolute percentage error (Testing) | | | | | | | 3.1356 |

## Testing of estimated model

Testing of the estimated model is performed with 11 disjoint data sets obtained from 11 separate follow up experimental runs conducted at the mid-level of feed rate. Testing results are shown in Table 7. The values of mean absolute percentage error (3.1356%) suggest the adequacy of the estimated model for application in practical field of work

## Optimization of Fd

Delamination of work surface always has a deleterious effect on quality of product performance. Thus, lower value of Fd is appreciable to the process engineers. Hence, optimum combination of input parameters (material thickness, drill diameter, spindle speed and feed rate) in drilling process to get minimum Fd in a certain working range is prerequisite in practical field of work. Here, modified PSO (as proposed in subsection 5.1) is applied on the developed SVM learned regression model [Eq. (18)] for searching optimum working condition satisfying minimum Fd within the pre-specified range (shown in Table 1). Control factors for modified PSO (n, ω, cog, soc, Ψ, iter $_{max}$, acc) are kept same as before. Initial position vectors and corresponding velocity vectors are randomly chosen within the specified search range.

Marching steps of the simulation process for minimization of Fd are shown in Fig. 13. Optimum results are shown in Table 8.

Coefficient of variation specifically signifies the relative measurement of spreading of the particles in swarm. Though CV value is dependent on random numbers, but the nature of change of this value somehow reflects the physical relationship among parameters and responses. Figure 14 indicates that components of position vector along feed rate, material thickness and spindle speed die down rapidly (that is CV decreases at faster rate), but

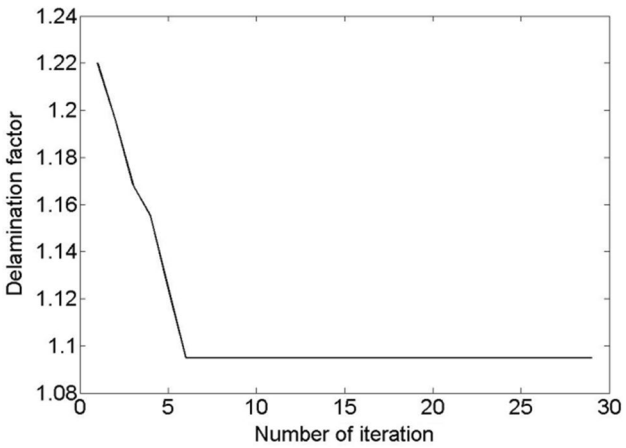


**Fig. 13** Marching steps for minimization of Fd

**Table 8** Optimum result and validation

| | Material thickness (mm) | Drill diameter (mm) | Spindle speed (rpm) | Feed rate (mm/rev) | Fd |
|---|---|---|---|---|---|
| Optimum | 16 | 14 | 1100 | 0.100 | 1.0949 |
| Experimental | 16 | 14 | 1100 | 0.100 | 1.1358 |
| Absolute % error | – | – | – | – | 3.6010 |

there is a gradual decaying nature in drill diameter component. Higher spindle speed and feed rate increase thrust force, which weakens the interplay bonding; as a result, separations of laminates occur. Also, thin material causes more push out delamination. So, change of drill diameter does not have too much influence on delamination, but

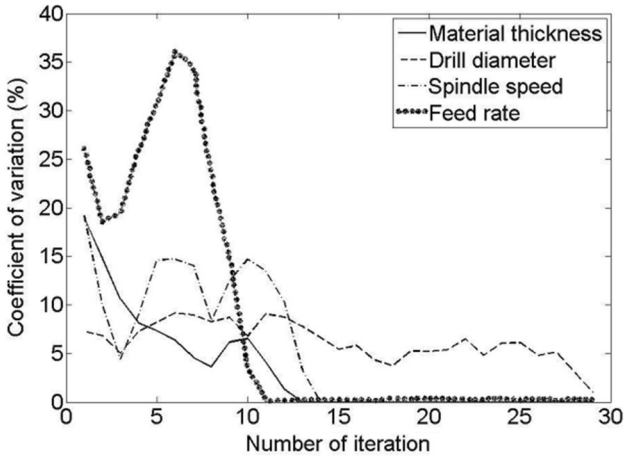


**Fig. 14** Change of CV along different dimensions with iteration for minimization of Fd

other three parameters—material thickness, spindle speed and feed rate effectively control quality of drilled product.

## Conclusions

Prediction of delamination factor of worksurface is very essential to fully diminish or decrease long-term product performance deterioration of glass fiber-reinforced polyester composites. Predictive model of the attribute is, therefore, prerequisite during the product development stage and freezing the design before final production. The glass fiber-reinforced polyester composite being an inhomogeneous and anisotropic material, small-scale variation in response is inevitable during drilling of this material. The developed SVM-based regression model with optimum parameter settings (C, $\varepsilon$ and $\sigma$) can efficiently capture the small-scale random fluctuations and can predict delamination factor of work surface for the material in a robust way. Validation result of estimated model favors the practical use of the model in the chosen range. Optimum combination of input parameters in drilling for minimum delamination factor is further found by applying modified particle swarm optimization technique on the developed model. Thus, a procedure is proposed that may be used effectively to develop model for this type of materials and determine optimal setting of input parameters.

## Appendix

See Table 9.

**Table 9** Difference of Lagrange multipliers ($\alpha_i$, $\alpha_i^*$) for Fd model (Training input vectors corresponding to # are the support vectors)

| Sl no. | Training input vector (mt, dd, ss, fr) | Difference of Lagrange multipliers for Fd model ($b=0$) ($C=2.1569$, $\varepsilon=0.0409$, $\sigma=0.8409$) |
|---|---|---|
| 1 | (8, 10, 400, 0.100) | 0.525195230090877# |
| 2 | (8, 10, 400, 0.175) | −0.000000002681717 |
| 3 | (8, 10, 400, 0.275) | 0.628536252568837# |
| 4 | (8, 10, 800, 0.100) | −0.000000001105429 |
| 5 | (8, 10, 800, 0.275) | −0.000000002767856 |
| 6 | (8, 10, 1100, 0.100) | 0.488347780417287# |
| 7 | (8, 10, 1100, 0.175) | −0.000000000923326 |
| 8 | (8, 10, 1100, 0.275) | 0.869153096157191# |
| 9 | (8, 12, 400, 0.100) | 0.000000000667942 |
| 10 | (8, 12, 400, 0.175) | −0.000000008090438 |
| 11 | (8, 12, 400, 0.275) | 0.000000003014198 |
| 12 | (8, 12, 800, 0.100) | 0.000000002772582 |
| 13 | (8, 12, 800, 0.275) | −0.000000002994774 |
| 14 | (8, 12, 1100, 0.100) | −0.000000000745200 |
| 15 | (8, 12, 1100, 0.175) | −0.191996378980079# |
| 16 | (8, 12, 1100, 0.275) | −0.000000000138956 |
| 17 | (8, 14, 400, 0.100) | 0.420717084163701# |
| 18 | (8, 14, 400, 0.275) | 0.753300692327161# |
| 19 | (8, 14, 800, 0.100) | −0.000000001120708 |
| 20 | (8, 14, 800, 0.275) | −0.000000002649887 |
| 21 | (8, 14, 1100, 0.100) | 0.955271411093371# |
| 22 | (8, 14, 1100, 0.175) | −0.341787963624719# |
| 23 | (8, 14, 1100, 0.275) | 0.728390996794064# |
| 24 | (12, 10, 400, 0.100) | 0.000000001589205 |
| 25 | (12, 10, 400, 0.175) | −0.035229314672588# |
| 26 | (12, 10, 400, 0.275) | 0.000000000549479 |
| 27 | (12, 10, 800, 0.100) | −0.000000014639496 |
| 28 | (12, 10, 800, 0.275) | −0.336788113630661# |
| 29 | (12, 10, 1100, 0.100) | 0.000000001427493 |
| 30 | (12, 10, 1100, 0.175) | −0.000000000880487 |
| 31 | (12, 10, 1100, 0.275) | 0.000000002899240 |
| 32 | (12, 12, 400, 0.100) | −0.000000005274340 |
| 33 | (12, 12, 400, 0.275) | −0.612166601421159# |
| 34 | (12, 12, 800, 0.100) | −0.262557292904846# |
| 35 | (12, 12, 800, 0.175) | −1.812426631063476# |
| 36 | (12, 12, 800, 0.275) | −0.003089092009327# |
| 37 | (12, 12, 1100, 0.100) | −0.000000001676854 |
| 38 | (12, 12, 1100, 0.275) | −0.349950619262231# |
| 39 | (12, 14, 400, 0.100) | −0.000000000377224 |
| 40 | (12, 14, 400, 0.175) | −0.000000005059569 |
| 41 | (12, 14, 400, 0.275) | 0.000000004844352 |
| 42 | (12, 14, 800, 0.100) | −0.000000000796432 |
| 43 | (12, 14, 800, 0.175) | −0.207664997506429# |
| 44 | (12, 14, 800, 0.275) | −0.014993484255197# |
| 45 | (12, 14, 1100, 0.100) | 0.000000005620053 |
| 46 | (12, 14, 1100, 0.175) | −0.000000000604029 |

**Table 9** (continued)

| Sl no. | Training input vector (mt, dd, ss, fr) | Difference of Lagrange multipliers for Fd model ($b=0$) ($C=2.1569$, $\varepsilon=0.0409$, $\sigma=0.8409$) |
|---|---|---|
| 47 | (12, 14, 1100, 0.275) | 0.000000000954048 |
| 48 | (16, 10, 400, 0.100) | 0.475054600075455# |
| 49 | (16, 10, 400, 0.275) | 0.935655046297500# |
| 50 | (16, 10, 800, 0.100) | −0.000000001468245 |
| 51 | (16, 10, 800, 0.175) | −0.075664319183429# |
| 52 | (16, 10, 800, 0.275) | 0.000000002074204 |
| 53 | (16, 10, 1100, 0.100) | 0.629697077003069# |
| 54 | (16, 10, 1100, 0.275) | 0.461344255770055# |
| 55 | (16, 12, 400, 0.100) | −0.000000001182409 |
| 56 | (16, 12, 400, 0.175) | −0.325956970076937# |
| 57 | (16, 12, 400, 0.275) | 0.000000000219459 |
| 58 | (16, 12, 800, 0.100) | −0.000000001131027 |
| 59 | (16, 12, 800, 0.275) | −0.000000000612663 |
| 60 | (16, 12, 1100, 0.100) | 0.000000002278166 |
| 61 | (16, 12, 1100, 0.175) | −0.000000003359762 |
| 62 | (16, 12, 1100, 0.275) | −0.000000001273847 |
| 63 | (16, 14, 400, 0.100) | 0.615913817680166# |
| 64 | (16, 14, 400, 0.175) | −0.000000000164384 |
| 65 | (16, 14, 400, 0.275) | 0.523060750010800# |
| 66 | (16, 14, 800, 0.100) | 0.000000000614136 |
| 67 | (16, 14, 800, 0.275) | −0.000000000552112 |
| 68 | (16, 14, 1100, 0.100) | 0.422506007138125# |
| 69 | (16, 14, 1100, 0.175) | −0.000000000151694 |
| 70 | (16, 14, 1100, 0.275) | 0.747454329697362# |

## References


1. Kilickap E (2010) Optimization of cutting parameters on delamination based on Taguchi method during drilling of GFRP composite. Expert Syst Appl 37(8):6116–6122
2. EI-Sonbaty I, Khasaba UA, Machaly T (2004) Factors affecting machinability of GFR/epoxy composites. Compos Struct 63(3–4):329–338
3. Callister WD Jr (2008) Callister's material science and engineering. Wiley, Bangalore
4. Capello E (2004) Workpiece damping and its effect on delamination damage in drilling thin composite laminates. J Mater Process Technol 148(2):186–195
5. Stone R, Krishnamurty K (1996) A neural network thrust force controller to minimize delamination during drilling of graphite-epoxy laminates. Int J Mach Tools Manuf 36(9):985–1003
6. Abrão AM, Faria PE, Rubio JCC, Reis P, Davim JP (2007) Drilling of fiber reinforced plastics: a review. J Mater Process Technol 186(1–3):1–7
7. Khashaba UA (2004) Delamination in drilling GFR-thermoset composites. Compos Struct 63(3–4):313–327
8. Abrão AM, Rubio JCC, Faria PE, Davim JP (2008) The effect of cutting tool geometry on thrust force and delamination when drilling glass fiber reinforced plastic composite. Mater Des 29(2):508–513
9. Velayudham A, Krishnamurthy K (2007) Effect of point geometry and their influence on thrust and delamination in drilling of polymeric composites. J Mater Process Technol 185(1–3):204–209
10. Rubio JC, Abrao AM, Faria PE, Correia AE, Davim JP (2008) Effects of high speed in the drilling of glass fiber reinforced plastic: evaluation of the delamination factor. Int J Mach Tools Manuf 48(6):715–720
11. Davim JP, Reis P, António CC (2004) Drilling fiber reinforced plastics (FRPs) manufactured by hand lay-up: influence of matrix (Viapal VUP 9731 and ATLAC 382-05). J Mater Process Technol 155–156:1828–1833
12. Davim JP, Reis P, António CC (2004) Experimental study on drilling glass fiber reinforced plastics (GFRP) manufactured by hand lay-up. Compos Sci Technol 64(2):289–297
13. Hocheng H, Tsao CC (2003) Comprehensive analysis of delamination in drilling of composite materials with various drill bits. J Mater Process Technol 140(1–3):335–339
14. Mohan NS, Kulkarni SM, Ramachandra A (2007) Delamination analysis in drilling process of glass fiber reinforced plastic (GFRP) composite materials. J Mater Process Technol 186(1–3):265–271
15. Palanikumar K, Prakash S, Shanmugam K (2008) Evaluation of delamination in drilling GFRP composites. Mater Manuf Processes 23(8):858–864
16. Khashaba UA, Seif MA, Elhamid MA (2007) Drilling analysis of chopped composites. Compos A Appl Sci Manuf 38(1):61–70
17. Karnik SR, Gaitonde VN, Rubio JC, Correia AE, Abrão AM, Davim JP (2008) Delamination analysis in high speed drilling of carbon fiber reinforced plastics (CFRP) using artificial neural network model. Mater Des 29(9):1768–1777
18. Bezerra EM, Ancelotti AC, Pardini LC, Rocco JAFF, Iha K, Ribeiro CHC (2007) Artificial neural networks applied to epoxy composites reinforced with carbon and E-glass fibers: analysis of the shear mechanical properties. Mater Sci Eng A 464(1–2):177–185
19. Palanikumar K (2011) Experimental investigation and optimization in drilling of GFRP composites. Measurement 44(10):2138–2148
20. Hsu I, Tsao CC (2008) Optimization of process parameters in drilling composite materials by Grey-Taguchi method. In: 8th Asia–Pacific conference on materials processing 2: 388-393
21. Benkedjouh T, Medjaher K, Zerouni N, Rechak S (2013) Health assessment and life prediction of cutting tools based on support vector regression. J Intell Manuf 1:1. https://doi.org/10.1007/s10845-013-0774-6
22. Gaitonde VV, Karnik SR (2012) Minimizing burr size in drilling using artificial neural network (ANN)- particle swarm optimization (PSO) approach. J Intell Manuf 23(5):1783–1793
23. Cristianini N, Taylor JS (2000) An Introduction to Support Vector Machines and other kernel-based-learning methods. Cambridge University Press, Cambridge
24. Breazak D, Majetic D, Udiljak T, Kasac J (2012) Tool wear estimation using an analytic fuzzy classifier and support vector machines. J Intell Manuf 23(3):797–809
25. Li DC, Chen WC, Liu CW, Lin YS (2012) A non-linear quality improvement model using SVR for manufacturing TFT-LCDs. J Intell Manuf 23(3):835–844
26. Çaydaş U, Ekici S (2012) Support vector machines models for surface roughness prediction in CNC turning of AISI 304 austenitic stainless steel. J Intell Manuf 23(3):639–650
27. Behera RR (2009) Simultaneous prediction of delamination and surface roughness in drilling GFRP composite using artificial neural network. ME Thesis, Jadavpur University
28. Aich U, Banerjee S (2014) Modeling of EDM responses by support vector machine regression with parameters selected by particle swarm optimization. Appl Math Model 38:2800–2818

29. Vapnik V (1995) The Nature of Statistical learning Theory. Springer, New York
30. Gunn SR (1998) Support vector machines for classification and regression. Technical report, University of Southampton
31. Smola AJ, Scholkopf B (2004) A tutorial on support vector regression. Stat Comput 14(3):199–222
32. Sapankevych N, Sankar R (2009) Time series prediction using support vector machines: a survey. IEEE Comput Intell Mag 4(2):24–38
33. Yu PS, Chen ST, Chang IF (2006) Support vector regression for real-time flood stage forecasting. J Hydrol 328(3–4):704–716
34. Levis AA, Papageorgiou LG (2005) Customer demand forecasting via support vector regression analysis. Chem Eng Res Des 83(8):1009–1018
35. Kennedy J, Eberhart R (1995) Particle swarm optimization. IEEE Int Conf Neural Netw 4:1942–1948
36. Hu X, Eberhart R (2002) Multiobjective optimization using dynamic neighborhood particle swarm optimization. Congr Evol Comput 2:1677–1681
37. Clerc M, Kennedy J (2002) The particle swarm: explosion, stability, and convergence in a multidimensional complex space. IEEE Trans Evol Comput 6(1):58–73
38. Tripathi PK, Bandyopadhyay S, Pal SK (2007) Multi-objective particle swarm optimization with time variant inertia and acceleration coefficients. Inf Sci 177(22):5033–5049
39. Tang Y, Wang Z, Fang J (2011) Parameters identification of unknown delayed genetic regulatory networks by a switching particle swarm optimization algorithm. Expert Syst Appl 38(3):2523–2535
40. Shi Y, Eberhart RC (1998) Parameter selection in particle swarm optimization. 7th International Conference on Evolutionary Programming VII 1447:591–600
41. Ratnaweera A, Halgamuge SK, Watson HC (2004) Self-organizing hierarchical particle swarm optimizer with time-varying acceleration coefficients. IEEE Trans Evol Comput 8(3):240–255
42. Cherkassky V, Ma Y (2004) Practical selection of SVM parameters and noise estimation for SVM regression. Neural Networks 17(1):113–126